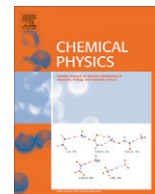




Contents lists available at ScienceDirect

Chemical Physics

journal homepage: www.elsevier.com/locate/chemphys

The thermodynamic cycle of an entropy-driven stepper motor walking hand-over-hand

Michał Żabicki^{a,*}, Werner Ebeling^b, Ewa Gudowska-Nowak^a

^a M. Smoluchowski Institute of Physics and M. Kac Complex Systems Research Center, Jagiellonian University, Reymonta 4, 30-059 Kraków, Poland

^b Institut für Physik, Humboldt Universität Berlin, Newtonstr. 15, 12489 Berlin, Germany

ARTICLE INFO

Article history:

Received 18 January 2010

In final form 2 June 2010

Available online xxxxx

Keywords:

Transport

Molecular motors

Efficiency

Kinesin

ABSTRACT

We develop a model of a kinesin motor based on an entropy-driven spring between the two heads of the stepper. The stepper is coupled to the energy depot which is reservoir of ATP. A Langevin equation for the motion of the two legs in a ratchet potential is analyzed by performing numerical simulations. It is documented that the model motor is able to work against a load force with an efficiency of about 10–30%. At a critical load force the motor stops to operate.

© 2010 Elsevier B.V. All rights reserved.

1. Introduction

Molecular motors are nano-machines operating under far-from thermal equilibrium conditions. In living cells molecular motors are complex protein assemblies that are capable of transforming chemical energy into work in order to perform various mechanical tasks, such as intracellular transport, ion pumping, DNA replication and protein synthesis [1,2]. In contrast to their macroscopic analogues designed by humans, biological molecular motors perform work in a noisy environment, where thermal fluctuations are significant and most likely, important to the operation of the motor.

Understanding basic principles of molecular motors functionality has been progressed over the past 20 years by design and analysis of relatively simple model systems whose action is determined by spatial/dynamic broken symmetry [3–6]. Most of those model systems describe molecular motors by a paradigm of a Brownian particle undergoing a random walk in a periodic asymmetric potential, and being acted upon by an external time-dependent force of zero average. Although the majority of the research in this field considers the presence of noise, several attempts have been made to model the transport properties of classical, deterministic and inertial ratchet systems [7–12]. These type of ratchets are known to generally display chaotic behavior within some regions of characteristic parameters. Accordingly, transport properties in those systems can be significantly influenced by the appearance of chaos. Moreover, rocked ratchets with massive particles are known to be

capable of reversing their current. Since the inertial effects make the rectification mechanism sensitive to the particle mass, this type of nano-devices exhibit properties of selective transport which can be used for segregation of mixed species.

Among the best known are biological motors [2,13] like kinesins and dyneins, which are able to take nanometre steps along protein tracks in the cytoplasm. These motors transport a wide variety of loads, power cell locomotion and when acting in large ensembles, allow organisms to move. Despite basic principles of motor-proteins design and mechanism have been derived [13–15], the detailed dynamics of these machines has not been fully understood yet. In particular, little is known about how motor-proteins bind to the proper cargo, become activated for transport, and deliver that cargo to the correct cellular target.

Molecular motors move along actin or microtubules by rapidly hydrolyzing ATP (adenosine triphosphate), a common biological energy source. It is generally accepted that motor binding to its filament greatly increases the rate of ATP hydrolysis, but the structural changes in the motor associated with ATPase activation are not known. There are also competing models for how the two-headed kinesin walks [16,14]. In the “inchworm” model, the leading head holds onto the microtubule, and the trailing head moves up to meet it. The second possibility is the “hand-over-hand” motion, in which the heads exchange leading and trailing roles with each subsequent step. By measuring the stepwise motion of individual enzymes the Block’s group has found [14] that some kinesin molecules exhibit a striking alternation in the dwell times between steps, causing these motors to “limp” along the microtubule. Such a limping pattern has been deduced to imply that kinesin molecules strictly alternate between two different

* Corresponding author.

E-mail addresses: zabicki@th.if.uj.edu.pl (M. Żabicki), ebeling@physik.hu-berlin.de (W. Ebeling), gudowska@th.if.uj.edu.pl (E. Gudowska-Nowak).

conformations as they step, indicative of an asymmetric, hand-over-hand mechanism.

In this paper we present the model for the inertia ratchet mimicking mechanism of the kinesin motion. We follow description of the stepping mechanism proposed by Bier [15,17] and derive a model of a thermodynamic machine which reflects basic characteristics of the Carnot cycle. An essential element in our model is the expansion and contraction of a polymer “spring” between two heads of the kinesin.

In our preliminary model for a molecular motor we include a term with inertia, typical for the underdamped Brownian motion. Consequently, we study more carefully the role of mass. In fact, when the particle receives momentum, it displaces the fluid in its immediate vicinity. The surrounding flow field is altered and acts back on the particle due to a non-negligible fluid inertia. The mass and the friction force then include additional terms that depend on the particles past motion, which leads to a hydrodynamic memory effect and a corrected form of the (non-Markovian) Langevin equation with a frequency-dependent friction. Such a hydrodynamic effect may delay the transition from ballistic to diffusive motion, resulting in a persistence of the nondiffusive motion to much longer times, as has been also supported by recent experiments [18].

However, in the context of biological motion, a small size of moving mechanical objects and the viscous drag force from the fluid environment are responsible for a fast equilibration of the motor velocity.¹ In effect, the viscosity dominates the inertia and velocity of the motor becomes proportional to force [13,15]. In order to fulfill this scenario, in the second part of the paper we present a modified version of the model based on separation of relative motion and center-of-mass motion. Within this approach, the inertia is irrelevant with respect to the center-of-mass motion and the latter is described by an overdamped Langevin equation.

2. Ideal thermodynamic models of the Carnot and the kinesin cycles

The Carnot cycle working on ideal gas is a metaphor for all motors working under isothermic–adiabatic conditions. Fig. 2 presents schematic diagrams of the Carnot cycle in the pressure–volume and in the energy–entropy spaces. In four steps of the Carnot cycle represented by two adiabats (isoentropic states) and two isotherms (isoenergetic states), the engine absorbs heat from hot reservoir, produces work and returns heat to the cold reservoir [19]. For an ideal gas the energy depends only on the temperature (and the particle number). In other words, the Carnot machine works between states characterized by two (constant) energies E_1 , E_2 and two (constant) entropies S_1 and S_2 . The efficiency of such a motor is defined by the ratio $\eta = W/Q$, where W is the total work done in a cycle in which the heat Q was absorbed. The Carnot's theorem states that reversible engines have the maximal efficiency given by $\eta = 1 - \frac{T_2}{T_1}$ where T_1 , T_2 characterize temperatures relevant for isothermal transitions (isothermal expansion of gas along upper curve and isothermal compression along lower curve in Fig. 1). Steps with constant entropies (S_1 , S_2) represent adiabatic compression and de-compression, respectively. In less efficient (irreversible) cycle, a smaller fraction of the heat absorbed is converted into work and efficiency drops, $\eta \leq 1 - \frac{T_2}{T_1}$.

An alternative representation of the idealistic cycle (note that internal energy can be scaled with temperature units) can be depicted in the energy–entropy (E, S) (or temperature–entropy) space

¹ The timescale of inertia is the time it takes for the motor to forget its current velocity due to friction. The inertial time scale for a 1- μm bead in water is estimated [2] to be ≈ 56 ns. Locomotion of a protein motor generally takes place on much longer time scales [13].

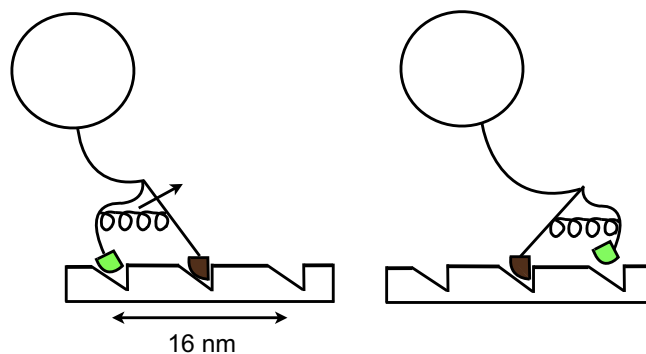


Fig. 1. A cartoon presentation of the kinesin motor stepping along the microtubule filament. As depicted, the kinesin is a dimer consisting of two units of about 350 amino acids [13]. When kinesin moves on a microtubule surface, it performs steps of amplitude 8.1 nm, the distance between adjacent tubulin binding sites. The steps are powered by the hydrolysis of ATP: each kinesin step involves “consumption” (power stroke) of about one ATP-molecule with a release of energy of about $13k_B T$.

in a form of a rectangular graph (see Fig. 2) with two pairs of parallel lines illustrating paths of transformations at constant energy and entropy, respectively. In what follows, we try to represent the mechanism of the kinesin motion [15] in a similar way, by adapting the scenario in which the movement of both heads is governed by entropic forces.

In Fig. 2, the Carnot cycle starts with a stage A of high energy, means high temperature of the gas. The gas expands isothermally in the following stage, increasing its entropy. Then the expansion

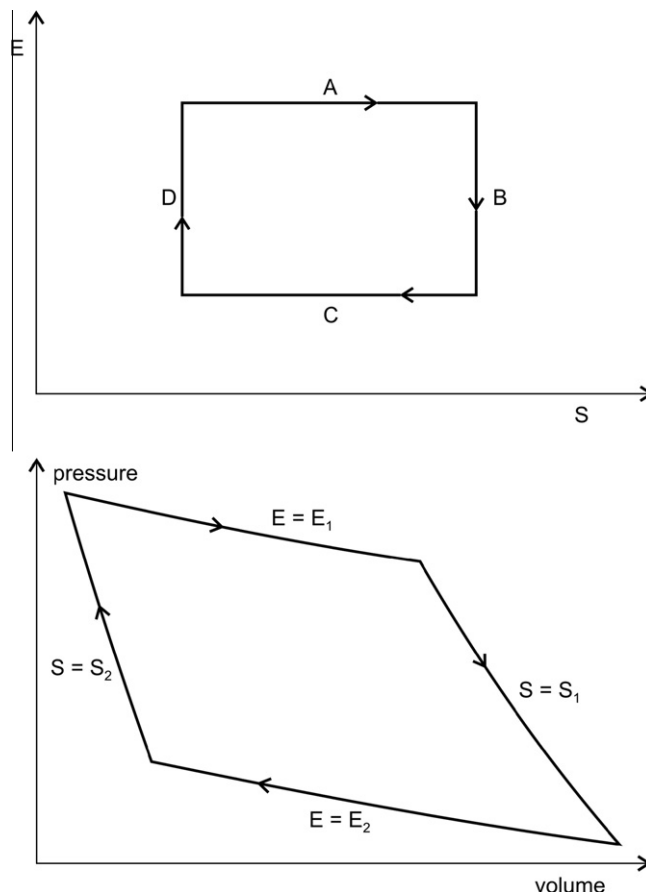


Fig. 2. Representation of the idealized Carnot cycle: in the internal energy versus entropy (E – S) diagram (above) and in the pressure–volume (p – V) diagram (below).

continues adiabatically in stage B at constant (but higher) entropy and the internal energy E decreases. In the next, third stage C, the energy remains constant at a lower level and the entropy goes down. Finally the low level entropy is reached and the compression continues in stage D, the energy increases.

The retracting tendency of a stretched polymer (or a rubber band linking two heads of the kinesin and holding them together) can be described in a similar manner: a polymer chain (consisting of tens of monomers) possesses a large number of possible conformations. With no external stretching force acting on the polymer strand, it will adopt one of (many) random-coil conformations. In consequence, if one holds two of the band ends at a fixed distance apart, the entropy of the system decreases when the distance increases. There must be an entropic force which opposes such stretching and this is exactly the retracting force which causes the stretched rubber to shrink again. Effectively, the retraction of a stretched polymer increases disorder and resembles the expansion of an ideal gas which also increases entropy and can perform real work.

The idealized kinesin stepper motor starts also in a state of high energy and low-entropy with the linker band stretched between its heads. Performing the motion requires the head to be first detached what causes loosening of the linking band and increases entropy. Figs. 1, 2, 5, and 6 explain how this thermodynamic scenario is working in a dynamic model which is explained below.

We assume kinesin to start its motion in a state (left upper corner of Fig. 2) where the heads are far apart, head 1 (brown) is in front and head 2 (pink) is behind. The spring is expanded and the entropy is low. In the first stage A the motor pulls the pink head out of its docking position and the spring, which is like a rubber band, is shortening. As the length of the elastomeric band decreases, the entropy of the system increases by ΔS .² The brown head remains at its position but the pink one continues to move up towards the flat hill of the ratchet. At this stage, corresponding to the transition B in Fig. 2, the entropy is still high but the internal energy of the motor drops by ΔE .

In the third stage C the pink head explores further the surface of the microtubule and hits eventually the next docking site. The band between the heads becomes stretched again and the entropy decreases. In stage D the pink head comes to rest, the rubber band is expanded, the entropy is low. Now the energy derived from the hydrolysis of one ATP-molecule allows next step to commence. The following cycle is taken over by the brown head. Altogether, the stepper resembles a two-hub motor. The analogy between a Carnot machine and a stepper motor, as described here, is entirely based on the role of energy and entropy.

Both cycles begin with a low-entropy state of the gas or the spring-molecule, respectively, then proceed to a high-entropy state and return cyclically to the low-entropy state. The role of energy is less transparent and schematically can be explained as follows: At first, after binding of an ATP to the rear head, a small portion of the energy is used for unlocking the chemical bond and loosening the stretch of the linker. The stretched configuration of the band is unique and corresponds to a low-entropy state. In contrast, detachment of the head is followed by a random coiling which increases available configurations. During detachment, stepping and eventual docking of the head at a new binding position, most of the ATP-energy becomes consumed. A new cycle starts with another act of energy absorption.

From the point of physics the two important steps in the thermodynamic model are:

² Note that for an ideal stretched elastomer the decrease in length corresponds to an increase of volume of an ideal gas. The first law of thermodynamics can be then written as $dE = TdS + F_S dx$ with an equation of state $F_S = k_B T f(\frac{x}{x^*})$, where x^* is the contour length in a worm-like-chain model for an unstructured polypeptide [20].

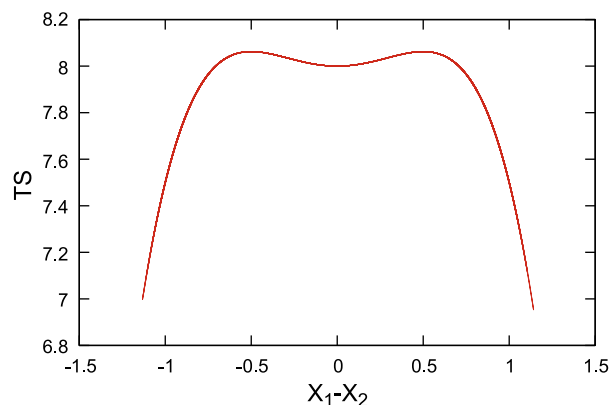


Fig. 3. An approximation of the rubber entropy as a function of the distance between the two heads of the motor. The middle part, which is essentially constant or has a small minimum, corresponds to the coiled state (maximal entropy) and the outer regions to the expanded rubber.

1. The energy support (absorption of an ATP-molecule) which starts the whole cycle.
2. The mechanism of a rubber band which serves as a depot of entropy.

Entropy of the rubber band is constant for $|x_1 - x_2| < s_0$ and decreases for $|x_1 - x_2| > s_0$ giving rise to a thermodynamic Onsager force expressed in terms of the derivative of the free energy potential

$$F_S(x) = - \left(\frac{\partial G}{\partial x} \right)_{\{y_i\}} = T \frac{dS}{dx} \quad (1)$$

where y_i stays for the set of constant thermodynamic parameters (like temperature T and pressure p).

For the purpose of modeling the motor movement, we use at first an analytic form of the entropy with a flat central region incorporating two small maxima³ (see Fig. 3)

$$TS(x) = s_0 + ax^2 - bx^4 \quad (2)$$

with the equilibrium distance $x^* = \sqrt{a/2b}$.

3. A dynamic model of the kinesin motor with two heads elastically coupled by a rubber band

More than 10 years ago a model of the dynamics of two-headed kinesin has been studied based on the idea that the heads are elastically coupled by a spring [5]. Our model follows the similar line of reasoning. As discussed in the former section, we first retain inertia in dynamic equations for the internal motion. This non-negligible effect of inertia is responsible, in turn, for a much richer dynamic scenario of the motor processivity. Additionally, we assume also that the force between the heads is nonlinear. In other words, the spring between the heads is replaced by a rubber band which creates a nonlinear thermodynamic force. Moreover, we introduce an additional element of an energy depot which stores the absorbed ATP-energy for certain time before it becomes transformed to mechanical energy of motion.

Such a model stays in a close relation to some recent studies of active Brownian dynamics on ratchet potentials [21,22] motivated

³ As a more realistic alternative, at least for an “ideal elastomer”, one could be tempted to use a piecewise-linear rubber band potential derived from the entropy $TS(x) = s_0$ for $|x| < x^*$ and $S(x) = s_0 - f|x - x^*|$ for $|x| > x^*$, which is, however, less suitable for extended numerical simulations. Additionally performed tests showed that our results are not sensitive to details of the entropy model.

by the work of Schweitzer et al. [23]. In the latter, the motion of particles is described by a Langevin equation for a generalized Rayleigh-oscillator. Incorporating the pumping of energy from the depot results in an acceleration of motion which has to be included in the basic equation describing the collective movement. Analysis of the active Brownian motion on ratchets indicates that the driving force in such systems is proportional to the velocity [23,21] and has a time dependence defined by an extra equation for a depot energy $e(t)$.

Generalizing the ansatz described in the papers [21,22], we model a kinesin stepper with two heads by formulating active Brownian motion for the positions of the two molecules representing the heads of the stepper (x_1, x_2), and for the energy content of the depot. For the sake of clarity, we start with equations including dimensions

$$m \frac{dv_1(t)}{dt} + m\gamma_0 v_1(t) + U'(x_1) - F_S(x_1 - x_2) = mde(t)v_1 - M\Gamma_0 \frac{dx_0(t)}{dt} + m\sqrt{2D_\nu}\xi_1(t) \quad (3)$$

$$m \frac{dv_2(t)}{dt} + m\gamma_0 v_2(t) + U'(x_2) - F_S(x_2 - x_1) = mde(t)v_2 - M\Gamma_0 \frac{dx_0(t)}{dt} + m\sqrt{2D_\nu}\xi_2(t) \quad (4)$$

$$\frac{de(t)}{dt} = q_0 - ce(t) - md(v_1^2 + v_2^2)e(t) \quad (5)$$

Here $U(x)$ is a ratchet-type potential representing the surface of the tubule with docking locations for the stepper, γ_0 is a friction frequency acting on the motion of the heads and Γ_0 is an additional friction frequency acting on the motion of the center of mass of the kinesin, including the load (cargo). The corresponding dissipative forces are $m\gamma_0 v_i$ and $Mv_0\Gamma_0$, whereas $F_S(x)$ represents the entropic force of an elastomer. Additional forces $\xi_1(t)$, $\xi_2(t)$ are independent, white Gaussian noises of intensity $m\sqrt{(2D_\nu)}$, where $D_\nu = \gamma_0 k_B T/m$. The coordinates x of molecular motion represent position of the heads (and the center of mass, respectively) on a one-dimensional structure of the track (tubule). The mechanical energy of motion is powered by the energy flow from the depot which depends on the coupling d . The energy accumulated in the depot container q_0 can be dissipated with a rate c . We assume that the position of the load is by distance s (the length of the rope) behind the center of the mass of two heads:

$$x_0(t) = \frac{1}{2}(x_1 + x_2) - \text{sgn}(v_1 + v_2)s \quad (6)$$

Now we have to decide about units to describe the processes in our systems. We introduce the unit length l_0 as the order of the period of the ratchet potential. Further, we introduce a characteristic time t_0 in such a way that the mass of the Brownian particle which is typically of the order of $m = (1-10) \times 10^{-19}$ g is normalized to one [24,25]. This can be achieved by introducing a unit of time by setting

$$t_0^2 = ml_0^2/E_0$$

Here E_0 is the unit of energy. This unit is still arbitrary, although as a convenient choice, we have decided to take a typical value for a biological activation energy ($E_0 \approx 0.1$ eV $\approx 1.602 \times 10^{-20}$ J ≈ 2.3 kcal/mol). We keep in mind that the value of one ATP-quantum gained in the process of hydrolysis is about 0.34 eV,⁴ i.e., it is about three times higher.

With this setting of units and by rescaling

$$\hat{x} = \frac{x}{l_0}, \quad \hat{t} = \frac{t}{t_0} \quad (7)$$

the dimensionless Langevin equations read:

$$\frac{d\hat{v}_1(\hat{t})}{d\hat{t}} + \gamma \hat{v}_1(\hat{t}) + \hat{U}'(\hat{x}_1) - \hat{F}_S(\hat{x}_1 - \hat{x}_2) = \hat{d}e(\hat{t})\hat{v}_1 - \Gamma \frac{d\hat{x}_0(\hat{t})}{d\hat{t}} + \sqrt{2D}\xi_1(\hat{t}) \quad (8)$$

$$\frac{d\hat{v}_2(\hat{t})}{d\hat{t}} + \gamma \hat{v}_2(\hat{t}) + \hat{U}'(\hat{x}_2) - \hat{F}_S(\hat{x}_2 - \hat{x}_1) = \hat{d}e(\hat{t})\hat{v}_2 - \Gamma \frac{d\hat{x}_0(\hat{t})}{d\hat{t}} + \sqrt{2D}\xi_2(\hat{t}) \quad (9)$$

$$\frac{d\hat{e}(\hat{t})}{d\hat{t}} = \hat{q} - \hat{c}e(\hat{t}) - \hat{d}(\hat{v}_1^2 + \hat{v}_2^2)e(\hat{t}) \quad (10)$$

with $\gamma = \gamma_0 t_0$, $\hat{U}' = U'/E_0$, $\hat{F}_S = F_S/E_0$, $D = \frac{m l_0}{E_0} D_\nu$, $\hat{d} = dt_0$, $\Gamma = M\Gamma_0 t_0/m$, $\hat{q} = q_0 t_0$ and $\hat{c} = ct_0$. For the sake of simplicity the notation with “hats” has been skipped in time and space variables, respectively. Altogether, Eqs. (8)–(10) resemble the driving mechanism of the Rayleigh-oscillator [26]. In our studies they are the starting point for modeling the head dynamics which includes both, inertia and external noise. Within this approach, the efficiency of the motor can be determined by the relation between the (net) power output and the power input q . Here the output is composed of the sum of work done (per time unit) by the stepper against the external force and the frictional energy loss by carrying the cargo across a viscous surroundings.

For the ratchet potential we used a standard model [27]:

$$U(x)/E_0 = -F_0 x + U_1(x) \quad (11)$$

$$U_1(x) = h \left[0.499 - 0.453(\sin(2\pi(x + 0.1903))) + \frac{1}{4}(\sin(2\pi(x + 0.1903))) \right] \quad (12)$$

where F_0 is an external biasing force directing to the left and h is the height (amplitude) of the barriers (in relation to E_0).

Already the first glance at the exemplary simulations (cf. Fig. 4) documents that the model exhibits the desired properties. For simulating trajectories described by Eqs. (8)–(10), we have assumed $F_0 = 0$, no external biasing force, but the existence of the load which has to be transported against friction ($\Gamma = 0.5$) and subsequent slopes of the periodic potential. The other parameter values have been taken from the model of unidirectional flow on a ratchet

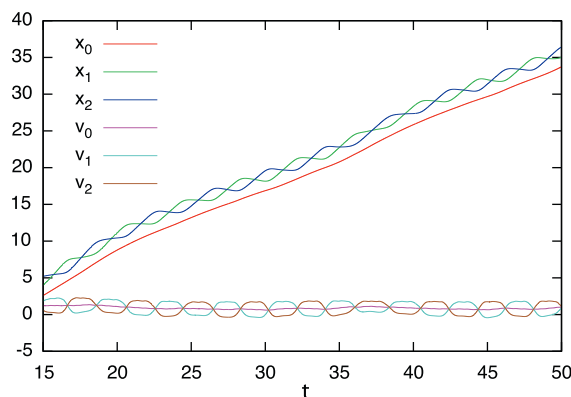


Fig. 4. Result of a simulation (Eqs. (8)–(10)) for the parameter set: $s_0 = 8$, $a = 0.5$, $b = 1$, $e = 0.1$, $h = 0.1$, $\gamma_0 = 0.02$, $q = 1.0$, $c = 0.1$, $d = 1$, $\Gamma = 0.5$, and $D = 0.25$. We show the positions of the two heads x_1 (green), x_2 (blue), the velocities of the heads $v_1(t)$ (light blue), $v_2(t)$ (brown). The position of the load x_0 is marked in red and its corresponding velocity v_0 is displayed in magenta. The time step of simulations, $\Delta t = 10^{-3}$. (For interpretation of the references to colour in this figure legend, the reader is referred to the web version of this article.)

⁴ At room temperature, $1k_B T = 0.0256$ eV $= 0.593$ kcal/mol.

analyzed elsewhere [28] and read $h = 0.1$, $q = 1$, $c = 0.1$, $d = 1$. For the coupling parameters of the nonlinear spring we have assumed $a = 0.5$, $b = 1$. The cycle displayed in Fig. 5 is a caricature of an idealized Carnot cycle and, as can be easily detected, represents consecutive steps of the stochastic process with time-variations in entropy and energy, cf. Fig. 6.

For time $t > 10$ the motion of the head-steppers is more or less stationary. On average, they carry the load in positive direction. However, the motion is influenced by stochastic effects and sometimes the head which stays behind, slides slightly back. Apart from some local stochastic irregularities, the velocities $v_1(t)$, $v_2(t)$ exhibit the pattern of bistability. The position of the load (the smooth line $x_0(t)$ in Fig. 4) stays always behind the position $(x_1 + x_2)/2$ of the center of mass (cf. Eq. (6)). The cargo is carried from left to the right against the friction that is made up of internal friction of the motor protein and of friction that occurs through interaction with the neighboring liquid medium. Altogether, the quasi-periodic time dependence of the entropy $S(t)$ and the depot energy $e(t)$ engaged in the motion are depicted in Fig. 5.

The efficiency η , is defined as the ratio of power $L(t)$ and the energy input rate. By assuming a bias force $F_0 = 0$, the efficiency can be derived from the formula

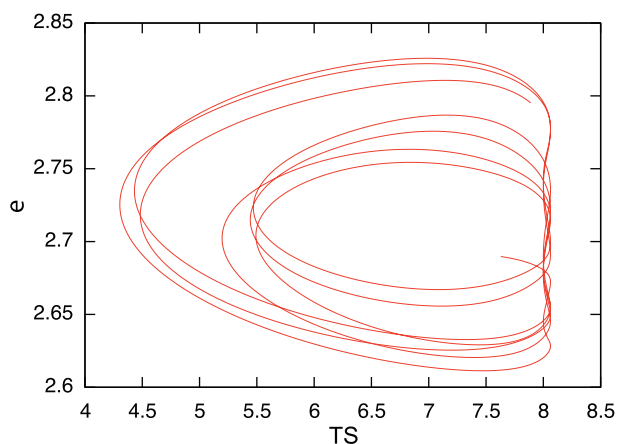


Fig. 5. The working cycle for the model of the kinesin motor displaying dependence between entropy of the elastic band and the depot energy $e(t)$. The parameters are $s_0 = 8$, $a = 0.5$, $b = 1$, $e = 0.1$, $h = 0.1$, $\gamma = 0.02$, $q = 1.0$, $c = 0.1$, $d = 1$, and $\Gamma = 0.5$. The time span: $t \in [55, 70]$.

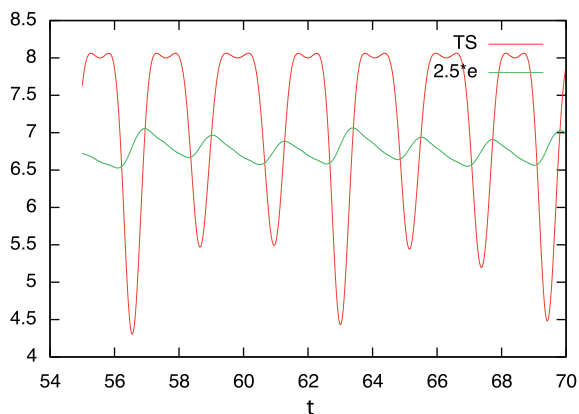


Fig. 6. Time-variations of the entropy $S(t)$ (red) and depot energy $e(t)$ (green) of the kinesin motor model described by Eqs. (8) and (9). Parameters of simulations as in Fig. 5. The scale of the variations $e(t)$ has been enlarged for clarity. (For interpretation of the references to colour in this figure legend, the reader is referred to the web version of this article.)

$$\eta = \left\langle \frac{L(t)}{q} \right\rangle \simeq \frac{\Gamma(v_0^2)}{q_0}$$

Corresponding to our simulations, the average speed of the center of mass is around $v_0 \simeq 0.8$. With $\Gamma = 0.5$, this yields efficiency of about 30%. Estimating the efficiency from the area of the Carnot cycle (cf. Fig. 5) gives the value of the same order. Note, however, that the loop area in Fig. 5 corresponds only to the part of the work as done by the rubber band connecting the heads of the motor and using the energy of the depot $e(t)$.

4. Separation of relative motion and center-of-mass motion

The rectifying properties of our model depend on the inertia terms in the dynamic Eqs. (8) and (9). To clarify this point we have investigated time-variations of the parameter $\zeta(t)$ representing the ratio between the inertia and the friction term, respectively:

$$\zeta(t) = \frac{|dv_i/dt|}{|\gamma v_i|} \quad (13)$$

Fig. 7 displays $\zeta(t)$ for the set of parameters relevant for detection of the directed current against the potential slope (cf. Fig. 4). Notably, the contribution of inertia as measured by the above relation Eq. (13) is rather large in course of time and dominates the dissipation term $\gamma v(t)$. Having in mind physical conditions under which molecular machines operate, we expect that internal motions may be underdamped but overall motions should be strongly damped according to the high friction occurring through the interaction with the environmental “fluid”.

In order to study this in more detail, we separate the relative and the center-of-mass motion, taking into account that mass and friction may be quite different for internal and external motion. Let us introduce center of mass coordinates and velocities

$$x = x_1 - x_2, \quad v = v_1 - v_2, \quad x_c = (x_1 + x_2)/2, \quad v_c = (v_1 + v_2)/2$$

Then by subtracting Eqs. (3) and (4) we get

$$\begin{aligned} \frac{mdv(t)}{dt} + m\gamma_c v(t) + (U'(x_c + x(t)/2) - U'(x_c - x(t)/2)) - 2TS'(x(t)) \\ = mde(t)v(t) + m\sqrt{2D_v}\xi(t) \end{aligned} \quad (14)$$

The corresponding dynamics for the energy reads

$$\frac{de(t)}{dt} = q - ce(t) - mdv^2e(t) \quad (15)$$

An analogous equation for the center of mass ($\gamma_c \equiv \gamma_0$, $\Gamma_c \equiv \Gamma_0$) is obtained by adding Eqs. (3) and (4). This way we get first

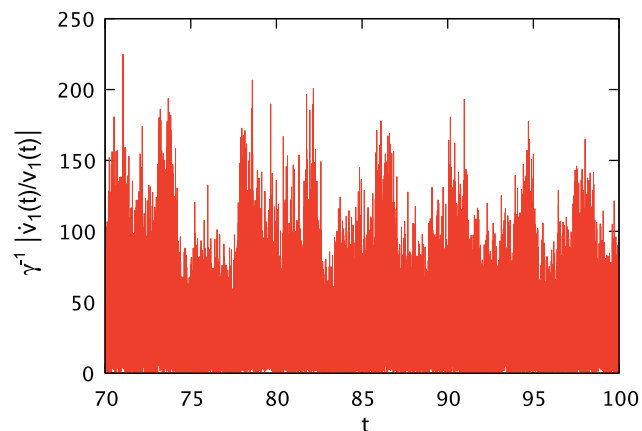


Fig. 7. The effect of inertia in the model described by Eqs. (8)–(12). The acceleration term $\dot{v}(t)$ is clearly dominant over the term $\gamma v(t)$ at most simulation times. The parameters of simulations are the same as in Fig. 4.

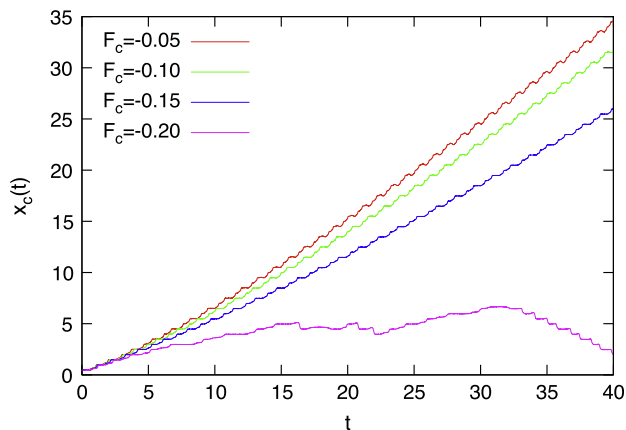


Fig. 8. Trajectories of the center of mass (above) for various values of the load force: $F_c = -0.05, -0.10, -0.15, -0.20$. At $F_c = -0.20$ the motor is already overloaded and ceases to operate at higher loads. Parameters for the simulation are $a = 0.5, b = 1, \gamma_c = 0.02, \Gamma = 0.2, q = 1.0, h = 0.1, c = 0.1, d = 0.1, D_{x_c} = 0.2$ and $D_v = 0.02$.

$$(2m) \frac{dv_c(t)}{dt} + (2m)\gamma_c v_c(t) + 2M\Gamma_c \frac{dx_c(t)}{dt} + (U'(x_c + x(t)/2) + U'(x_c - x(t)/2)) = (2m)de(t)v_c(t) + (2m)\sqrt{2D_v}(\xi_1(t) + \xi_2(t))/2 \quad (16)$$

Now we introduce several physical assumptions:

- (i) We neglect the terms including the mass of the heads in comparison to terms with the total mass of the kinesin.
- (ii) We introduce a center-of-mass noise, corresponding to the center-of-mass friction $\Gamma = 2M\Gamma_c$ and an external force F_c acting at the center of mass. Due to the relations

$$x_1 = x_c + x/2, \quad x_2 = x_c - x/2 \quad (17)$$

the equation of motion of the center of mass may be written as

$$\frac{dx_c(t)}{dt} = \frac{F_c}{\Gamma} - \frac{1}{\Gamma} [(U'(x_c + x(t)/2) + U'(x_c - x(t)/2))] + \sqrt{2D_{x_c}}\xi_0 \quad (18)$$

i.e., in consequence of the above assumptions, we end up with an overdamped equation of motion for the center of mass. Note that this is in part derived from Eqs. (3)–(5) with an additional (ad hoc) postulate that the mass and the friction of the complex are not “simple” (additive) functions of two masses and two friction coefficients representative for the motion of the heads.⁵

Accordingly, in the simulations we can use now $\Gamma \gg \gamma_c$. As a result, v_c will be much smaller and can be adapted to a more realistic molecular speed.

As it is demonstrated in Fig. 8, the adapted ratchet still operates and is able to perform work against a force driving to the left, assuming that this force is not too large. For a given set of parameters, the mechanism of the hand-over-hand transport seems to break down for $-F_c > 0.2$. By defining the efficiency of performing work against the external force F_c as $\eta = \frac{|F_c v_c|}{q}$, we find that for the cases of motion displayed in Fig. 8 the efficiencies are lower than for a preliminary model of an inertia ratchet (cf. Section 3) and reach only about 10%. In our working examples we have obtained

efficiencies which first increase with a load force up to $\eta = 0.10$ for $F_c = -0.15$ and then drop to $\eta = 0$ at $F_c = -0.2$. This observation is in line with experimental data [32] which show similar behavior of the efficiency versus the load F_c with a maximal load at which the machine is still able to operate, $F_c = 8$ pN.

5. Conclusions

In this work we have introduced a functional model of a motor-molecule whose driving is powered by entropic forces [15]. A cartoon model of a stepper motor is composed of two heads linked by a rubber band. The motor performs hand-over-hand motion, expanding and contracting the rubber band in subsequent steps. Two versions of the model have been discussed. In a first version where all friction terms are rather small, the efficiency reaches up to 30%. In other words, this motor model needs inertia in order to function. However, due to small molecular size of the motor, in most biological applications the viscous forces are overtaking the inertia effects and the overdamped dynamics is a valid approximation [1,4,13]. Following this line of reasoning, in a second part of the paper we have introduced a motor model in which only the internal motion includes inertia, whereas the motion of its center of mass becomes overdamped. In such a model the efficiency is worse and reaches only about 10% at the load $F_c = -0.10$. Here, the estimated energetic efficiency has been defined as the ratio of the power to the (chemical) energy (ATP quanta) input rate. Preliminary analysis of this function against the load carried by the motor displays a strongly non-monotonous behavior (first increase of the efficiency with the load force up to a maximum, followed by a decrease to zero) in accordance with experimental data for kinesin [32] and former theoretical models of inertial Brownian motors [24,31].

Entropic forces have been rarely discussed in the context of nanomechanical devices [33,34], although entropy-functional units might be easier controllable by external parameters (like temperature or external fields) and their motion induced without changing the chemical structure of the components. Therefore the design of such entropy-driven systems seems to be of particular interest in the field of engineering of artificial motors for nano-scale transport.

Acknowledgements

This project has been supported in part by the ESF program Exploring Physics of Small Devices (EPSD) and has operated within the Foundation for Polish Science co-financed by the European Regional Development Fund covering, under the Agreement No. MPD/2009/6, the Jagiellonian University International Ph.D. Studies in Physics of Complex Systems.

The authors acknowledge many stimulating discussions with M. Bier and L. Schimansky-Geier.

The paper has been dedicated to Peter Hänggi on the occasion of his 60th birthday anniversary.

References

- [1] P. Nelson, Biological Physics, W.H. Freeman and Company, New York, 2008.
- [2] C. Bustamante, D. Keller, G. Oster, Acc. Chem. Res. 34 (6) (2001) 412.
- [3] R.D. Astumian, M. Bier, Phys. Rev. Lett. 72 (1994) 1766.
- [4] M. Bier, Phys. Rev. Lett. 91 (14) (2003) 148104.
- [5] I. Derényi, T. Vicsek, Proc. Natl. Acad. Sci. USA 93 (13) (1996) 6775.
- [6] M.O. Magnasco, Phys. Rev. Lett. 71 (10) (1993) 1477.
- [7] M. Kostur, P. Hänggi, P. Talkner, J. Mateos, Phys. Rev. E 72 (2005) 036210.
- [8] M.O. Vincent, Acta Phys. Pol. B 38 (2007) 2459.
- [9] W.-S. Son, J.-W. Ryu, D.-U. Hwang, S.-Y. Lee, Y.-J. Park, C.-M. Kim, Phys. Rev. E 77 (2008) 066213.
- [10] H. Hagman, C. Dion, P. Sjlund, S. Petra, M. Kastberg, Europhys. Lett. 81 (2008) 33001.
- [11] P. Jones, M. Goonasekera, F. Renzoni, Phys. Rev. Lett. 93 (2004) 073904.

⁵ Considering that $x(t)$ is a periodic function of time, the new overdamped dynamics reminds very much the scenario of flashing ratchets [29,30] in which the intriguing phenomenon of the negative mobility has been observed [24,31].

- [12] T. Prager, L. Schimansky-Geier, I. Sokolov, *J. Phys.: Condens. Matter* 17 (2005) S3661.
- [13] J. Howard, *Mechanics of Motor Proteins and the Cytoskeleton*, Sinauer Associates, Sunderland, 2001.
- [14] S. Block, *Biophys. J.* 92 (2007) 2986.
- [15] M. Bier, *Contemp. Phys.* 46 (1) (2005) 41.
- [16] N. Carter, R. Cross, *Nature* 435 (2005) 308.
- [17] M. Bier, *The energetics*, *Biosystems* 93 (2008) 23.
- [18] B. Lukić, S. Jeney, C. Tischer, A. Kulik, L. Forró, E. Florin, *Phys. Rev. Lett.* 95 (2005) 160601.
- [19] D. Kondepudi, *Introduction to Modern Thermodynamics*, John Wiley and Sons, Chichester, 2008.
- [20] P. Scherer, S. Fischer, *Theoretical Molecular Biophysics*, Springer-Verlag, Berlin, 2010.
- [21] W. Ebeling, E. Gudowska-Nowak, A. Fiasconaro, *Acta Phys. Pol. B* 39 (5) (2008) 1251.
- [22] A. Fiasconaro, E. Gudowska-Nowak, W. Ebeling, *J. Stat. Mech.: Theory Exp.* (2009) P01029.
- [23] F. Schweitzer, W. Ebeling, B. Tilch, *Phys. Rev. Lett.* 80 (1998) 5044.
- [24] L. Machura, M. Kostur, P. Talkner, J. Luczka, F. Marchesoni, P. Hänggi, *Phys. Rev. E* 70 (2004) 061105.
- [25] L. Machura, M. Kostur, J. Luczka, *Biosystems* 94 (2008) 253.
- [26] F. Schweitzer, W. Ebeling, B. Tilch, *Phys. Rev. Lett.* 80 (1998) 5044.
- [27] J. Mateos, *Acta Phys. Pol. B* 32 (2) (2001) 307.
- [28] A. Fiasconaro, W. Ebeling, E. Gudowska-Nowak, *Eur. Phys. J. B* 65 (3) (2008) 403.
- [29] P. Reimann, *Phys. Rep.* 361 (2002) 57.
- [30] B. Lindner, L. Schimansky-Geier, P. Reimann, P. Hänggi, M. Nagaoka, *Phys. Rev. E* 59 (1999) 1417.
- [31] L. Machura, M. Kostur, P. Talkner, J. Luczka, P. Hänggi, *Phys. Rev. Lett.* 98 (2007) 040601.
- [32] M. Nishiyama, H. Higuchi, T. Yanagida, *Nat. Cell Biol.* 4 (2002) 11782.
- [33] A. Hanke, R. Metzler, *Chem. Phys. Lett.* 359 (2002) 22.
- [34] A. Goel, V. Vogel, *Harnessing biological motors to engineer systems for nanoscale transport and assembly*, *Nat. Nanotechnol.* 3 (2008) 465.